Medical Mycology Case Reports 44 (2024) 100641

Contents lists available at ScienceDirect

Medical Mycology Case Reports

journal homepage: www.elsevier.com/locate/mmcr

Disseminated *Rasamsonia argillacea* complex infection presenting as intraventricular brain hemorrhage in a German shepherd dog in Australia

Christopher Skinner [a,*], Rachel Allavena [b], Karon Hoffmann [c], Mirrim Kelly-Bosma [b], Sarah Kidd [d], Christine Thomson [a]

[a] Animal Referral Hospital, 532 Seventeen Mile Rocks Road, Sinammon Park QLD 4073, Australia
[b] School of Veterinary Science, The University of Queensland, Gatton Campus, Gatton QLD 4343, Australia
[c] Imaging Vets, PO Box 3055, Putney NSW 2112, Australia
[d] National Mycology Reference Centre, Microbiology and Infectious Diseases, SA Pathology, Frome Road, Adelaide SA 5000, Australia

ARTICLE INFO

Handling Editor: Dr Adilia Warris

Keywords:
Systemic mycosis
MRI
Geosmithia
Talaromyces
Angiotropism

ABSTRACT

A German Shepherd Dog diagnosed with *Rasamsonia argillacea* based on fungal culture and DNA sequencing, is the first documented case in Australia, and the Southern Hemisphere. This species is part of *R. argillacea* complex, which is an emerging concern in immunocompromised human and veterinary patients. Intraventricular brain hemorrhage, noted on MRI, has not been reported previously in a dog with fungal encephalitis. The patient was euthanized due to progression of clinical signs before a final diagnosis was made, so no treatment was attempted in this case.

1. Introduction

Rasamsonia argillacea complex infection was first diagnosed in 2009 and can cause chronic granulomatous disease in humans and animals. After its original discovery in 1969, it went through a series of name changes (*Geosmithia argillacea* and *Talaromyces eburneus*) and is now described as Rasamsonia species complex comprising *R. argillacea*, *R. piperina*, *R. aegroticola* and *R. eburnea* [1–3].

Rasamsonia argillacea complex, are thermophiles associated with hot environments [3], but thus far, have only been *identified* as pathogenic in humans and animals in the northern hemisphere [4,5] with no previous reports in humans or animals in the southern hemisphere.

Disseminated mycoses, including by *Rasamsonia*, generally occur in immunocompromised humans and animals, [6,7]. German shepherd dogs (GSD), especially females, are overrepresented for disseminated mycoses [8], which may be due to an inherited abnormality in IgA and/or mucosal immunity dysfunction [9]. However, not all dogs with disseminated mycoses have low serum IgA, so the underlying mechanism of infection appears to be more complex [7,10].

Systemic mycosis due to *R. argillacea* complex causing has been reported in 11 cases in dogs seven of which were in GSDs in the UK and USA [7,11–13]. Affected animals had clinical signs in various body systems including nervous, respiratory, cardiovascular, musculoskeletal, gastrointestinal, lymphatic, and urinary systems.

Intraventricular brain hemorrhage (IVH) has not been reported in previous veterinary fungal encephalitis cases including reports of *R. argillacea* complex. In humans, IVH is associated with increased morbidity and mortality rates, and a poor prognosis [14,15].

This case report documents both the first case of disseminated fungal infection due to the *R. argillacea* complex in the southern hemisphere, and fungal-associated, intraventricular brain hemorrhage in a dog.

2. Case

In November 2020, A 7-year-old, female spayed German Shepherd Dog, weighing 35kg, presented to the Animal Referral Hospital in Brisbane, Australia, for acute onset ataxia and collapse. The episode lasted about 30 seconds, during which her eyes were ‘darting left and right’, and she was non-ambulatory for about 2 min.

On initial presentation, day 0, the dog had a low head carriage, mild postural reaction deficits in the right pelvic limb and multifocal spinal hyperpathia (cervical and thoracolumbar). She went on to develop anisocoria and had an episode of altered mentation. Mannitol was administered an hour prior to induction of general anesthesia for a

* Corresponding author.
E-mail address: C.Thomson@arhvets.com (C. Skinner).

https://doi.org/10.1016/j.mmcr.2024.100641
Received 20 February 2024; Accepted 1 March 2024
Available online 8 March 2024

contrast-enhanced, MRI using a 1.5 T MRI (Siemens, Sempra). The following changes were identified (see Fig. 1): obstructive hydrocephalus at the level of the obex, causing tetraventriculomegaly, hemorrhagic sediment in the lateral ventricles, in the right lateral aperture of the fourth ventricle and in the cranial, cervical subarachnoid space. Meningeal enhancement was noted both within the caudal fossa and the cranial cervical meninges. Cerebrospinal fluid (CSF) sampling was not performed at this time due to evidence of raised intracranial pressure. An abdominal ultrasound was performed by an internal medicine specialist, identifying mild splenic changes only. Coagulation testing identified hyperfibrinogenemia, leading to concern for a hemorrhagic disorder affecting the nervous system.

Due to the decline in pain management despite opioid analgesia on day 3, and newly identified retinal hemorrhage, lumbar CSF sampling was performed, which revealed marked inflammation with an eosinophilic component (see Table 1). Samples of CSF and serum were forwarded to the University of Sydney, School of Veterinary Science, for additional testing. *Toxoplasma* and *Neospora* titres (IgG/M) were negative in CSF and serum samples. Quantitative PCR testing was performed on CSF and was weakly positive for *Angiostrongylus cantonensis* at high PCR cycle number. The dog was discharged in the evening on day 6, but shortly after returning home became ambulatory tetraparetic, ataxic, restless, withdrawn, vocalizing, and anorexic. Following readmission on day 7, the dog became pyrexic (39.5 °C), and on day 9 she developed a positional vertical nystagmus.

On the morning of day 11, the dog remained pyrexic and became dull, tetraplegic, had intermittent nystagmus, and multifocal spinal hyperpathia. The dog also became tachycardic, tachypneic with increased respiratory effort, had a mucoid nasal discharge, and developed a corneal ulcer in the left eye, which was confirmed by fluorescein staining. The owners elected for discharge; however, she presented to the emergency and critical care service a few hours later after becoming cyanotic, developing a persistent rotary nystagmus, and more severe tachypnoea. The owner elected for humane euthanasia. Additional results of diagnostic testing including reference values and treatment are supplied in Table 1.

Post-mortem examination revealed extensive lesions, most of which were attributed to a systemic mycosis, upon discovery of fungal hyphae on histopathology. The most impressive and chronic lesions were observed in the kidney (Fig. 2a), with similar lesions in the spleen, and included necrotising granulomatous vasculitis resulting in nephritis and splenitis with the intralesional fungal hyphae. In the spleen there was a substantial infarct secondary to the vasculitis. Pulmonary lesions were characterised by locally extensive hemorrhage. Macroscopically, brain and spinal cord lesions included severe, acute, segmental, subarachnoid hemorrhage, moderate, subacute ventricular distension, and intraventricular hemorrhage (Fig. 2b and c), and moderate, chronic geriatric dural fibrosis, which was considered incidental. Histopathologic examination identified widespread pyogranulomatous meningitis with hemorrhage in the leptomeninges of the brainstem, cerebellum, and cerebrum. There was also direct fungal invasion with granulomatous inflammation of the cerebellar folia. The fungus was visible when stained with Grocott's methenamine silver, but not on hematoxylin and eosin-stained sections. The fungus was strongly angiotrophic for arterial and venous lumens, walls, and perivascular tissue and was present within granulomatous inflammation in the organ parenchyma. It was characterised as being hyphal, septate, with acute angle, dichotomous branching, and parallel walls, 3–6 μm wide with some 15-μm bulbous dilations (Fig. 3). The intraventricular hemorrhage was confirmed on histopathology, however choroid plexus within examined sections had normal morphology, and the site of hemorrhage was not identified despite extensive dissection and examination. The spinal cord also exhibited leptomeningeal, granulomatous inflammation and hemorrhage, noted in all segments of the cord examined from the cervical, thoracic, and lumbar regions. Prominent hemorrhage was present within the central canal of the cervical and thoracic spinal cord. Granulomatous radiculitis was identified in a large ventral nerve root in the lumbar region. Other changes identified included severe, acute diffuse megaesophagus. Moderate hyperplastic arteriosclerosis of the large pulmonary vessels, with some peribronchial mineralisation was also noted. This was chronic and attributed as a sequela to a previously treated *Dirofilaria immitis* infection, as heartworm can cause pulmonary hypertension. Additional findings included multifocal fibroid intervertebral disc disease (Hansen Type II) with mild spondylosis.

Samples were sent to the National Mycology Reference Centre in South Australia. Fungal culture on Sabouraud dextrose agar at 30 °C, grew flat, pale cinnamon-colored colonies with a brown reverse (Fig. 4 a and b), after 7 days. Inspection of the microscopic morphology revealed penicillus-like monoverticillate and biverticillate conidiophores with finely roughened walls, elongated phialides bearing cylindrical to ovoidal shaped conidia, somewhat resembling a *Penicillium* or *Paecilomyces* species (Fig. 4c). DNA sequencing of the internal transcribed spacer (ITS1-5.8S-ITS2) regions of the ribosomal DNA [16] was performed with pairwise sequence comparison using the BLAST algorithm against the MycoBank (www.mycobank.org) and GenBank (https://blast.ncbi.nlm.nih.gov/Blast.cgi) databases, revealing a 99.8% match to *R. argillacea*.

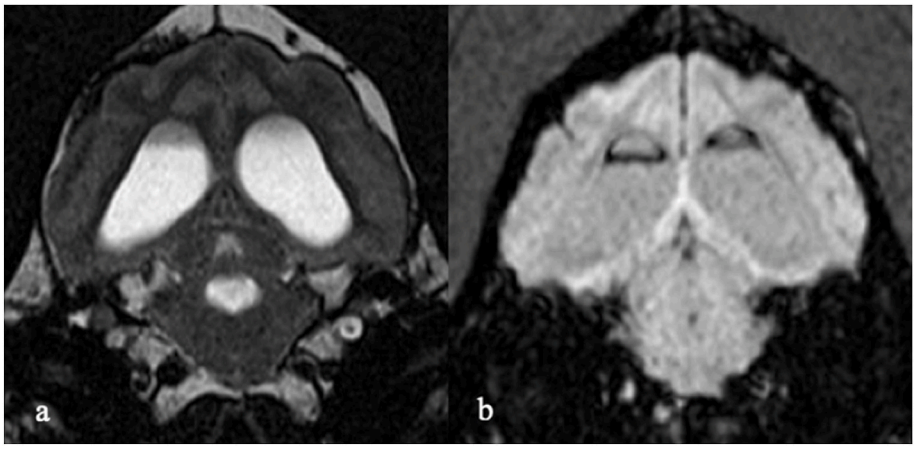

Fig. 1. MR images in the transverse plane at the level of the fourth ventricle and cochlea. (a) T2-weighted imaging and (b) susceptibility weighted imaging (SWI). The patient was in dorsal recumbency. The lateral ventricles are enlarged, containing areas of dependent material. (a) T2-weighted heterogeneously hypointense material in the dependent, dorsal part of the ventricles compared to the hyperintense cerebrospinal fluid. (b) Susceptibility artefact (arrowhead) in the dependent material, consistent with blood products.

Table 1
treatments and diagnostic test results during hospitalization (for blood test results, only abnormal findings included).

	Treatments	Diagnostic Test Results
Day 0	Methadone 0.3mg/kg SC	CBC - eosinophils 1.82x10^9/L (0.06–1.23), basophils 0.12x10^9/L (0.00–0.10) Biochemistry – globulins 52g/L (25–45) PT = WNL aPTT = WNL
Day 1	Methadone 0.3mg/kg q6h SC Levetiracetam 20mg/kg q8h PO Mannitol 0.5g/kg IV Dexamethasone 0.1mg/kg q24h IV Hartmann's solution 3ml/kg/hr	MRI summary – obstructive hydrocephalus at the level of the obex causing tetraventriculomegaly, hemorrhagic sediment in lateral ventricles + olfactory recess of the left lateral ventricle + right lateral aperture of fourth ventricle + cranial cervical subarachnoid space, meningeal enhancement in caudal fossa and cranial cervical spinal cord. Ophthalmic exam – suspected OS chorioretinitis
Day 2	Methadone 0.3mg/kg q6h SC Levetiracetam 20mg/kg q8h PO Mannitol 0.5g/kg IV Dexamethasone 0.1mg/kg q24h IV Hartmann's solution 3ml/kg/hr	PT = WNL aPTT = WNL Thrombin time 23s (11.0–17.0) Fibrinogen 4.43g/L (1.00–2.50) CBC – leukocytes 24.5x10^9/L (6.0–14.0), neutrophils 20.8x10^9/L (4.1–9.4), monocytes 2.5x10^9/L (0.2–1.0), eosinophils 0.00x10^9/L (0.1–1.2) Abdominal ultrasound – hypoechoic nodule in tail of spleen causing capsular distortion, smaller nodule in body of spleen cranial to the tail, otherwise unremarkable
Day 3	Methadone 0.3mg/kg q6h SC Mannitol 0.5g/kg IV Dexamethasone 0.1mg/kg q24h IV Clindamycin 15mg/kg q12h IV Pregabalin 2.1mg/kg q12h PO Hartmann's solution 3ml/kg/hr	CSF lumbar cistern – NCC 7100x10^6/L (<6 x 10^6/L), RCC 98000x10^6/L (5.65–8.87 x10^12/L), protein 2.93g/L (<0.45 g/L), 59% neutrophils, 19% monocytes and macrophages (with erythrophagia), 16% small lymphocytes, 6% eosinophils, occasional plasma cells Neurological PCR (*Toxoplasma gondii* DNA, *Neospora caninum* DNA, Cryptococcus spp. DNA, Angiostrongylus spp. DNA, Canine Distemper virus RNA) = negative PT = WNL aPTT = WNL Ophthalmic exam – OS ventral fundus mild perivascular retinal hemorrhage
Day 4	Methadone 0.3mg/kg q6h SC Prednisolone 0.57mg/kg q12h PO Clindamycin 12.9mg/kg q12h PO Pregabalin 2.1mg/kg q12h PO Omeprazole 0.57mg/kg q12h PO Fenbendazole 50mg/kg q24h PO	Repeat *Angiostrongylus cantonensis* quantitative PCR at the University of Sydney = weak positive *Toxoplasma gondii* antibody titres (CSF + serum) = negative *Neospora caninum* antibody titres (CSF + serum) = negative
Day 5	Methadone 0.3mg/kg q8h SC Prednisolone 0.57mg/kg q12h PO Clindamycin 12.9mg/kg q12h PO Pregabalin 2.1mg/kg q12h PO Omeprazole 0.57mg/kg q12h PO Fenbendazole 50mg/kg q24h PO	Nil
Day 6	Prednisolone 0.57mg/kg q12h PO Clindamycin 12.9mg/kg q12h PO Pregabalin 2.1mg/kg q12h PO Omeprazole 0.57mg/kg q12h PO Fenbendazole 50mg/kg q24h PO	Nil
Day 7	Prednisolone 0.86mg/kg q24h PO Omeprazole 0.57mg/kg q12h PO Trimethoprim sulphonamide 17.1mg/kg q12h PO Fenbendazole 50mg/kg q24h PO	Nil
Day 8	Prednisolone 0.86mg/kg q24h PO Omeprazole 0.57mg/kg q12h PO Trimethoprim sulphonamide 17.1mg/kg q12h PO Clindamycin 12.9mg/kg q12h PO Aminocaproic acid 14.3mg/kg q8h PO Fenbendazole 50mg/kg q24h PO	CBC – leukocytes 18.2x10^9/L (6.0–14.0), neutrophils 16.4x10^9/L (4.1–9.4) Biochemistry – alkaline phosphatase 277 U/L (1–120), tT4 <6nmol/L (22–49)
Day 9	Prednisolone 0.86mg/kg q24h PO Omeprazole 0.57mg/kg q12h PO Pregabalin 2.1mg/kg q12h PO Trimethoprim sulphonamide 17.1mg/kg q12h PO Methadone 0.3mg/kg q6h SC Aminocaproic acid 14.3mg/kg q8h PO Clindamycin 12.9mg/kg q12h PO Fentanyl 2.9mcg/kg TD	Nil
Day 10	Prednisolone 0.86mg/kg q24h PO Omeprazole 0.57mg/kg q12h PO Pregabalin 2.1mg/kg PO (morning dose) Pregabalin 2.9mg/kg PO (evening dose) Trimethoprim sulphonamide 17.1mg/kg q12h PO Aminocaproic acid 14.3mg/kg q8h PO Clindamycin 12.9mg/kg q12h PO Fentanyl 2.9mcg/kg TD Fentanyl CRI 2mcg/kg/hr Ketamine 10mcg/kg/min	Nil
Day 11	Prednisolone 0.86mg/kg q24h PO Omeprazole 0.57mg/kg q12h PO Pregabalin 2.9mg/kg q12h PO Aminocaproic acid 14.3mg/kg q8h PO Fentanyl 2.9mcg/kg TD Amoxiclav 500mg q12h PO Tricin q6h OS	Fluorescein stain uptake = positive OS, negative OD

3. Discussion

To the author's knowledge, this is the first reported case of *Rasamsonia argillacea* infection in Australia, and in the Southern Hemisphere in the veterinary or human literature. *Rasamsonia argillacea* is part of a

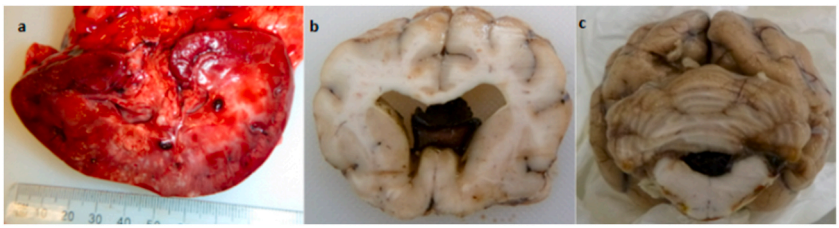

Fig. 2. Gross necropsy images: a) cut surface of renal pelvis depicting necrotising, granulomatous lesion occupying the renal pelvis and extending into the parenchyma (arrowheads). b) Transverse section of the brain at the level of the caudate nuclei, depicting ventricular dilation and hemorrhage (dark material) within the lateral ventricles. c) Transverse section of the brain at the level of the cerebellum depicting hemorrhage (dark material) within the fourth ventricle and lateral apertures. Size bars 1 cm.
Should be printed in color.

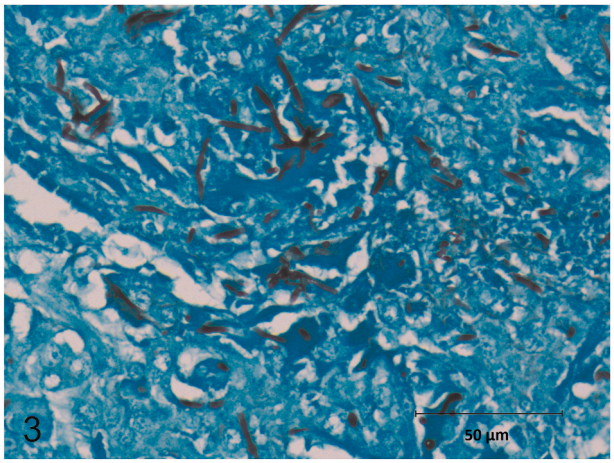

Fig. 3. Histological image of the cerebellum, Gomori's methanamine silver stain, depicting fungal hyphae in the cerebellum. Size bar = 50 µm.
Should be printed in color.

group of fungal species called *Rasamsonia argillacea* species complex. This case is also novel in its presentation of intraventricular hemorrhage, which we could not find previously reported in a dog with fungal encephalitis.

Rasamsonia argillacea species complex is an emerging pathogen in human medicine, particularly for immunocompromised patients including those with cystic fibrosis and chronic granulomatous disease [1] and has been reported has been reported in 11 case reports in dogs [1,7,11,12,15], in which the German Shepherd breed predominates (7/11 cases). Like *Aspergillus, R. argillacea* appears to have a vascular tropism, with granulomatous lesions localized around blood vessels in patients. *Rasamsonia* spp. Closely resemble *Aspergillus* in histopathologic section, displaying septate hyphal walls and dichotomous branching [2]. Without fungal identification in this case, a diagnosis of aspergillosis may have been wrongly assumed based on the histomorphology of fungal hyphae, the signalment of this case and distribution of lesions. As the cultured fungal morphology was not specific, DNA sequencing was performed. Previous cases of *R. argillacea* species complex may have been misclassified as *Paecilomyces* spp. or *Penicillium* spp. due to similarities in morphologic appearance [4,15]. This highlights the importance of DNA sequencing for correct specimen identification in dogs with disseminated mycosis. Clinical signs in this dog indicated involvement of the nervous and cardiopulmonary systems. This compares similarly to previous case reports from the northern hemisphere, which documented involvement of multiple body systems The novelties of this case were intraventricular hemorrhage, subarachnoid hemorrhage, and geographical location of Australia and, thereby, the Southern Hemisphere.

Acute decompensation after about one week of hospitalization was

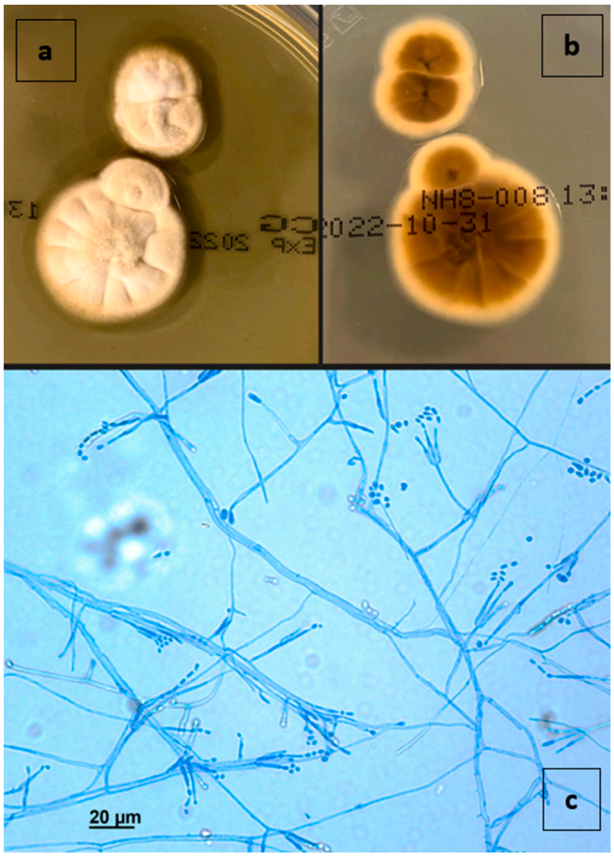

Fig. 4. Colony and microscopic morphology of *Rasamsonia argillacea* isolate. Colony morphology from top (a) and reverse aspects (b). Microscopic morphology from a culture preparation stained with lactophenol cotton blue and imaged at 400X magnification (size bar 20 μm (c).
Should be printed in color.

associated with dullness and increased respiratory rate and effort. At the time, parasitic infection with angiostrongyliasis or dirofilariasis was considered, however, clear evidence of either infection was lacking, so only symptomatic treatment was given. Acute decompensation occurred again on day 11, at which point owners elected euthanasia. Post-mortem examination identified moderate, chronic regionally extensive hemorrhage, thought to be secondary to either vasculitis or unidentified mycosis; this was suspected to be the primary cause for respiratory decompensation. Other chronic pulmonary changes were thought to be due to *Angiostrongylus cantonensis* and/or *Dirofilaria immitis* infection and may have reduced the dog's ability to compensate when fungal related hemorrhage occurred. Three previous cases in dogs had macroscopic pulmonary or pleural involvement but only one of these cases had

cytological evidence of fungal hyphae, making it unclear if there is a predisposition to develop respiratory disease or if this is secondary to vascular disease [7,12].

Retinal hemorrhage observed in the left eye, prompted performance of coagulation tests such as PT, aPTT, fibrinogen and hematological analysis. The dog was found to have hyperfibrinogenaemia, suggesting systemic inflammation, but normal PT and aPTT. Eosinophilia and hyperglobulinemia were identified initially (both of which have been associated with systemic mycoses [15]), while subsequently the dog developed neutrophilia and monocytosis, (interpreted as either systemic inflammation or a stress leukogram).

The spinal hyperpathia found on examination of this dog was presumed due to marked, chronic intervertebral disc disease, granulomatous meningitis, and/or leptomeningeal hemorrhage, all of which were noted on post-mortem examination. A few days after presentation the dog's cervical pain worsened, which is likely secondary to progressive, leptomeningeal hemorrhage. Interestingly, no evidence of diskospondylitis was found in this dog, which was found in several previous reports of *R. argillacea* species complex infection [2,11,12], and in one study was found radiographically in just over half of canine disseminated aspergillosis cases [6].

Along with multifocal spinal hyperpathia the dog initially presented with anisocoria, pelvic limb ataxia and proprioceptive deficits, which could have been associated with ocular, spinal cord, or cerebellar involvement.

While gross pathological changes in the kidney were noted, sufficient renal function remained for the lesions to be subclinical. Retrospectively, assessment of concentrated urinary sediment may have led to an antemortem diagnosis of fungal infection. The spleen also had similar lesions to the kidney, which again was unlikely to have much clinical significance. Dissemination of the fungi to the brain and spinal cord resulted in most of the clinical signs, with both cerebellar parenchymal infection, vasculitis, and extensive spinal leptomeningeal hemorrhage and radiculitis. Although not microscopically examined, the megaesophagus may have been associated with fungal invasion of the esophageal nerve supply (vagus nerve and/or recurrent laryngeal nerves) causing dysfunction. The origin of intraventricular hemorrhage was not identified, and the choroid plexus sections examined had no sign of infection or hemorrhage. It is possible that areas of choroid plexus not examined were damaged or, potentially, the hemorrhage originated from the meningeal or parenchymal vessels and circulated in the cerebrospinal fluid (CSF) to the ventricles.

It is thought that IVH contributed significantly to the clinical signs reported in this patient, by increasing ventricular volume and, therefore, intracranial pressure. No specific treatment for IVH was administered to the dog in this case study, rather it was treated with corticosteroids with the aim to reduce inflammation and, potentially, CSF production. One treatment for IVH is deferoxamine, an iron chelating agent, which has been shown to reduce hemorrhagic and ischemic brain injury in rats and piglets with intracerebral hemorrhage [13]. Thrombolytic agents have also been demonstrated to increase clearance of IVH with faster normalisation of ventricular volume [17]. Ventricular dilation also may be due to blockage of CSF circulation by blood clots, and/or general increase in fluid volume with the addition of blood to the CSF.

The data in veterinary and human literature on successful treatment of *Rasamsonia* spp. infections are limited. Antifungal susceptibility profiles in one study were similar in most strains of *R. argillacea* species complex. Caspofungin, an echinocandin, was the most active antifungal agent, followed by amphotericin B and posaconazole [3,15]. Itraconazole and voriconazole had variable susceptibility profiles [4,17]. Unfortunately, this patient was diagnosed with systemic mycosis by post-mortem examination and subsequent fungal culture and DNA sequencing, therefore treatment was not attempted, and susceptibility testing was not performed.

A commercially available real-time PCR assay (Primerdesign™, UK) was validated in one study for accurate detection of *R. argillacea* complex in humans [18]. Specifically, it was validated for three of the four species of *R. argillacea* species complex that typically affect humans with cystic fibrosis including *R. argillacea*, *R. piperina* and *R. aegroticola*. This study found that the real-time PCR assay had a higher sensitivity and was more rapid than culture-based methods. This test is commercially available and may be useful in cases of suspected systemic mycosis for earlier identification of *R. argillacea* species complex.

This case report demonstrates an unusual presentation of disseminated *R. argillacea* species complex infection in a GSD. Fungal associated, intraventricular hemorrhage, and *R. argillacea* species complex infection in Australia have not been published in the human or veterinary literature. This is important for future cases of systemic mycosis in both humans and veterinary patients in Australia, as accurate identification of the correct etiologic agent will improve patient outcomes. It is possible that previous infections may have been misclassified based on similar histomorphology of fungal hyphae to other fungal species, with no reports in the human or veterinary literature prior to Grant and others in 2009. There are no previous reports of fungal disease resulting in intraventricular hemorrhage, so this adds a new differential diagnosis that should be considered in any future cases of IVH. Real-time PCR assays for *R. argillacea* species complex are commercially available and could lead to more rapid diagnosis and improved patient outcome if utilized.

Funding

This research did not receive any specific grant from funding agencies in the public, commercial, or not-for-profit sectors.

Conflict of interest

The authors have no conflicts of interest to disclose.

4. Aurhor statement

Christopher Skinner: Conceptualisation, Software, Investigation, Resources, Writing – original draft, Visualisation. Christine Thomson: Conceptualisation, Methodology, Validation, Investigation, Resources, Data Curation, Writing – review & editing, Visualisation, Supervision, Project administration, Funding acquisition. Rachel Allavena: Validation, Formal Analysis. Karon Hoffman: Validation, Formal Analysis. Mirrim Kelly-Bosma: Validation, Formal Analysis. Sarah Kidd: Validation, Formal Analysis.

Acknowledgements

There are no acknowledgements.

References

[1] S. Giraud, L. Favennec, M.E. Bougnoux, J.P. Bouchara, Rasamsonia argillacea species complex: taxonomy, pathogenesis and clinical relevance, Future Microbiol. 8 (8) (2013) 967–978.
[2] D. Grant, D. Sutton, C. Sandberg, R. Tyler Jr., E. Thompson, A. Romanelli, B. Wickes, Disseminated Geosmithia argillacea infection in a German Shepherd dog, Med. Mycol. J 47 (2) (2009) 221–226.
[3] J. Houbraken, S. Giraud, M. Meijer, S. Bertout, J.C. Frisvad, J.F. Meis, J. P. Bouchara, R.A. Samson, Taxonomy and antifungal susceptibility of clinically important Rasamsonia species, J. Clin. Microbiol. 51 (1) (2013) 22–30.
[4] T. Matos, T. Cerar, M. Praprotnik, U. Krivec, M. Pirs, First recovery of Rasamsonia argillacea species complex isolated in adolescent patient with cystic fibrosis in Slovenia – case report and review of literature, Mycoses 58 (8) (2015) 506–510.
[5] A. Mouhajir, O. Matray, S. Giraud, L. Mély, C. Marguet, I. Sermet-Gaudelus, S. Le Gal, F. Labbé, C. Person, F. Troussier, J.J. Ballet, G. Gargala, R. Zouhair, M. E. Bougnoux, J.P. Bouchara, L. Favennec, Long-term Rasamsonia argillacea complex species colonization revealed by PCR amplification of repetitive DNA sequences in cystic fibrosis patients, J. Clin. Microbiol. 54 (11) (2016) 2804–2812.
[6] R.M. Schultz, E.G. Johnson, E.R. Wisner, N.A. Brown, B.A. Byrne, J.E. Sykes, Clinicopathologic and diagnostic imaging characteristics of systemic aspergillosis in 30 dogs, J. Vet. Intern. Med. 22 (4) (2008) 851–859.

[7] J. Lodzinska, P. Cazzini, C. Taylor, J. Harris, S. Kilpatrick, T. Liuti, G. Paterson, Systemic Rasamsonia piperina infection in a German shepherd cross dog, JMM Case Rep. 4 (10) (2017) 10–13.
[8] E. Cook, E. Meler, K. Garrett, H. Long, K. Mak, C. Stephens, A. Thompson, Disseminated Chrysosporium infection in a German shepherd dog, Med Mycol Case Rep 2015 10 (2015) 29–33.
[9] M. Olsson, M. Frankowiack, K. Tengvall, P. Roosje, T. Fall, E. Ivansson, K. Bergvall, H. Hansson-Hamlin, K. Sundberg, A. Hedhammar, K. Lindblad-Toh, L. Hammarstrom, The dog as a genetic model for Immunoglobulin A (IgA) deficiency: identification of several breeds with low serum IgA concentrations, Vet. Immunol. Immunopathol. 160 (3–4) (2014) 255–259.
[10] J. Stephen, E.C.F. Ettinger, Chapter 234: aspergillosis – canine, in: fifth ed. Textbook of Veterinary Internal Medicine: Diseases of the Dog and Cat, W.B. Saunders Co, Philadelphia, 2000, p. 1039.
[11] R. Salgüero, A.M. Borman, M. Herrtage, G. Benchekroun, E. Abbondati, V. Piola, A. Vanhaesebrouck, Rasamsonia argillacea mycosis in a dog: first case in Europe, Vet. Rec. 172 (22) (2013) 581–583.
[12] L. Kawalilak, A. Chen, G. Roberts, Imaging characteristics of disseminated Geosmithia argillacea causing severe diskospondylitis and meningoencephalomyelitis in a dog, Clin Case Rep 3 (11) (2015) 901–906.
[13] J.D. Dear, K.L. Reagan, S.E. Hulsebosch, C. Li, M.J.L. Munro, B.A. Byrne, V. K. Affolter, N. Wiederhold, C. Canete-Gibas, J.E. Sykes, Disseminated Rasamsonia argillacea species complex infections in 8 dogs, J. Vet. Intern. Med. 35 (5) (2021) 2232–2240.
[14] Z. Chen, C. Gao, Y. Hua, R. Keep, K. Muraszko, G. Xi, Role of iron in brain injury after intraventricular hemorrhage, Stroke 42 (2) (2011) 465–470.
[15] H. Hinson, D. Hanley, W. Ziai, Management of intraventricular hemorrhage, Curr Neurol Neurosci Repp 10 (2) (2011) 73–82.
[16] T.J. White, T.D. Bruns, S.B. Lee, J.W. Taylor, Amplification and direct sequencing of fungal ribosomal RNA Genes for phylogenetics, in: PCR Protocols: A Guide to Methods and Applications, Academic Press Inc, New York, 2012, pp. 315–322.
[17] J. Dai, S. Li, X. Li, W. Xiong, Y. Qiu, The mechanism of pathological changes of intraventricular hemorrhage in dogs, Neurol. India 57 (5) (2009) 567–577.
[18] J. Steinmann, S. Giraud, D. Schmidt, L. Sedlacek, A. Hamprecht, J. Houbraken, J. F. Meis, J.P. Bouchara, J. Buer, P.M. Rath, Validation of a novel real-time PCR for detecting Rasamsonia argillacea species complex in respiratory secretions from cystic fibrosis patients, New Microbes New Infect 2 (3) (2014) 72–78.